

Synthesis, optical and electrochemical properties of new thieno[2,3-*b*]indole-based dyes

Artur N. Bakiev,^{a*} Roman A. Irgashev,^{d,e} Elena V. Shklyueva,^{b,c} Aleksandr N. Vasyanin,^b
George G. Abashev,^{a,b} Gennady L. Rusinov,^{d,e} and Valery N. Charushin^{d,e}

^a Institute of Technical Chemistry, Ural Division of the Russian Academy of Sciences,
Ac. Koroleva Str. 3, Perm 614 990, Russia

^b Perm State University, Bukireva Str. 15, Perm 614 990, Russia

^c Institute of Natural Sciences of Perm State University, Genkel Str. 4, Perm 614990, Russia

^d Postovsky Institute of Organic Synthesis, Ural Division of the Russian Academy of Sciences,
Kovalevskaya Str. 22 / Akademicheskaya Str. 20, Ekaterinburg 620 990, Russia

^e B. N. Yeltsin Ural Federal University, Mira Str. 19, Ekaterinburg 620 002, Russia
E-mail: gabashev@psu.ru

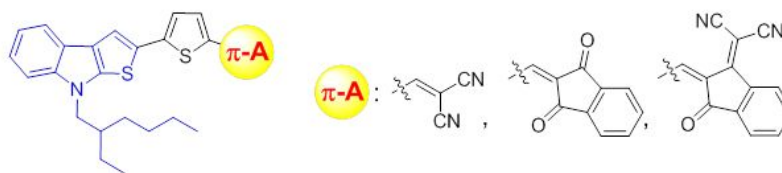
Received 12-25-2017

Accepted 03-02-2018

Published on line 05-31-2018

Abstract

Three new push-pull dyes consisting of a thieno[2,3-*b*]indole ring system as an electron donor, thiophene spacer as a π -bridge, and electron-withdrawing moieties such as 2-methylene malonitrile, 2-methylene-1*H*-indene-1,3(2*H*)-dione, and 2-(2-methylene-3-oxo-2,3-dihydro-1*H*-inden-1-ylidene)malononitrile, have been synthesized and studied for their application in organic electronics devices. Investigation of their optical and electrochemical properties reveal that these compounds possess narrow band gaps (1.7-2 eV) and an effective absorption in the visible spectral range (440-740 nm). Therefore, these chromophores can be regarded as promising light-harvesting materials.



Keywords: Thieno[2,3-*b*]indoles, thiophene-2-carbaldehydes, isatins, Knoevenagel condensation, push-pull structures, chromophores, light-harvesting dyes

Introduction

Small π -conjugated organic molecules bearing pyrrole and thiophene rings are the focus of acute attention due to their promising applications as electro- and photo-luminescent, charge-transport and light-harvesting materials for high-performance electronic devices such as organic light-emitting diodes (OLEDs), organic field-effect transistors (OFETs), and organic photovoltaic cells (OPVs).¹⁻⁵ Nevertheless, literature data concerning the applications of π -conjugated compounds based on thieno[3,2-*b*]indole and thieno[2,3-*b*]indole (TI) subunits as active components for organic photovoltaic (OPV) devices are rather limited. For example, two series of push-pull metal-free dyes containing the electron-rich carbazole (**MK 1-8**)⁶⁻⁷ and thieno[3,2-*b*]indole (**MKZ 39-41**)⁸ moieties (Fig. 1) have been synthesized, studied and further used as effective sensitizers for high-performance dye-sensitized solar cells (DSSC).

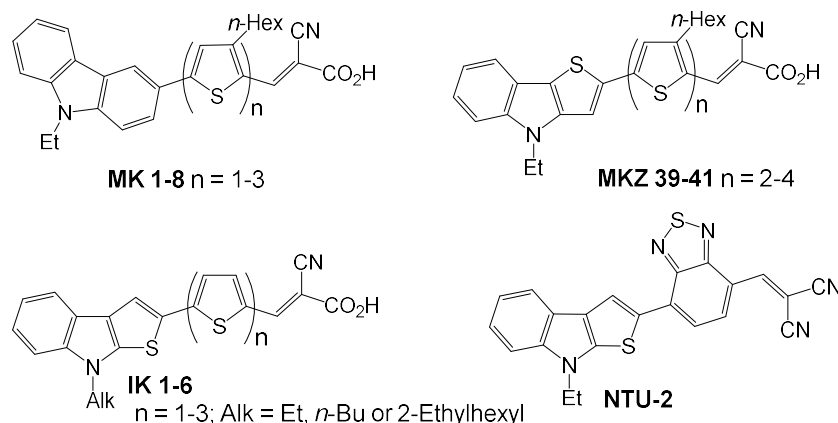


Figure 1. Structures of carbazole- and thienoindole-based dyes for OPVs.

Recently, we have reported a convenient two-step synthetic approach to construct 2-(hetero)aryl-substituted thieno[2,3-*b*]indoles using the corresponding acetylated (hetero)arenes and 1H-indole-2,3-dione (isatin) derivatives as starting compounds.⁹ Furthermore, 2-thien-2-yl-substituted thieno[2,3-*b*]indoles were successfully applied for preparation of the **IK 1-6** series of dyes (Fig. 1). The DSSCs based on these sensitizers have exhibited power-conversion efficiencies (PCE) up to 6.3%.^{10,11} It has also been reported that the planar and bulk heterojunction solar cells (HSC) based on a donor-acceptor couple, consisting of the **NTU-2** dye (Fig.1) as an electron-donor, light-harvesting component, and C₇₀-fullerene as an electron-acceptor component, also exhibited high PCE values of 5.2%.¹² Therefore, the incorporation of the thieno[2,3-*b*]indole fragment as an electron-donating subunit into the π -conjugated systems for use as new photo- and electro-active organic materials, and their further investigation, appear to be important issues for the field of organic photovoltaics.

Results and Discussion

Herein, we report convenient syntheses of three new thieno[2,3-*b*]indole-based D- π -A chromophores, and the investigation of their photophysical and electrochemical properties. The key stages of the reaction procedures are outlined in Figure 2. 5-{8-(2-Ethylhexyl)-8H-thieno[2,3-*b*]indole-2-yl}thiophene-2-carbaldehyde (**1**) was prepared in three steps from the synthetically available 1-(2-ethylhexyl)isatin and 2-acetylthiophene according to the previously described procedures.^{9,11} Chromophores **2-4** were synthesized via Knoevenagel condensation

of the thienaldehyde (**1**) with malononitrile, indan-2,3-dione and 2-(3-oxo-2,3-dihydroindene-1-ylidene)malononitrile, respectively. It has been found that this aldehyde readily reacts with malononitrile in refluxing glacial acetic acid in the presence of pyrrolidine as a base to yield (**2**), while the reaction of indan-2,3-dione with its respective derivatives proceeds smoothly by heating under reflux in ethanol to yield (**4**) and *n*-butanol to yield (**3**), and does not require any basic catalyst.^{13,14} More detailed descriptions of the processes used to prepare aldehyde (**1**) and 3-(dicyanomethylidene)indan-1-one are presented in the Supplementary Material section.

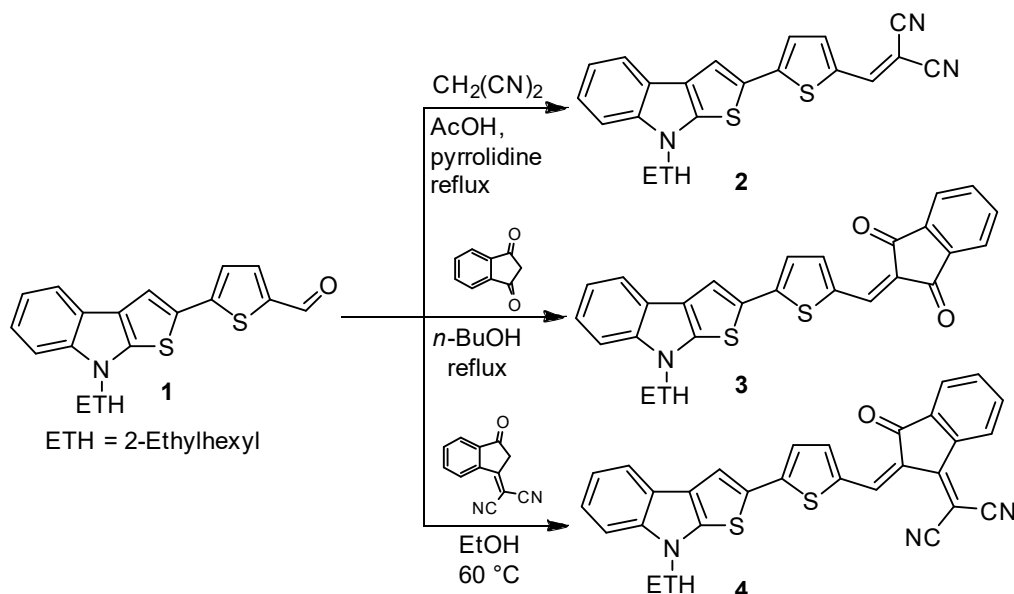


Figure 2. Key stages in syntheses of TI-based dyes **2-4**.

UV-vis absorption and fluorescence spectra of compounds **2-4** were recorded for their CHCl_3 solutions ($2 \times 10^{-5} \text{ mol L}^{-1}$). The corresponding absorption and fluorescence spectra are presented in Figure 3 and the results are summarized in Table 1. The main absorption bands in the visible region of 440-740 nm, with high molecular-absorption coefficients, correspond to the intramolecular charge-transfer (ICT) transitions proceeding in a dye molecule, whereas the absorption bands in the 240-440 nm region can be attributed to the $\pi\text{-}\pi^*$ transitions.

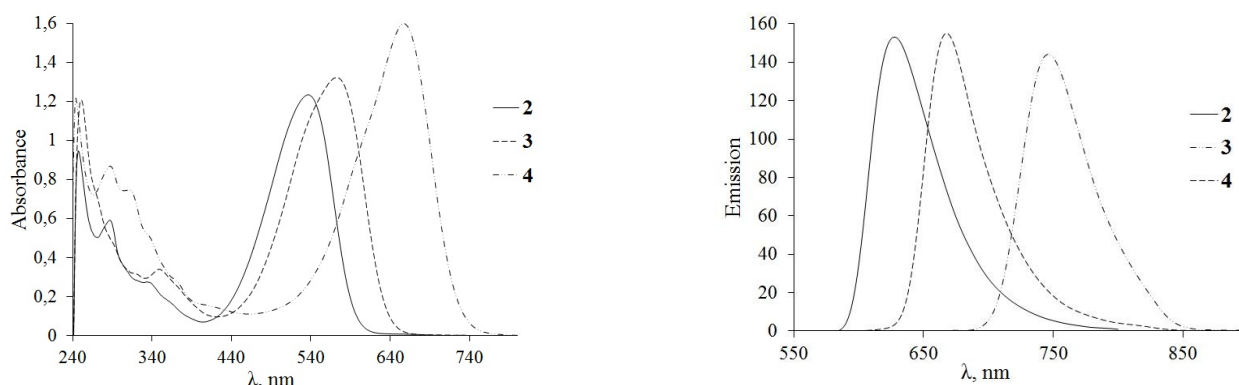
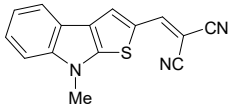
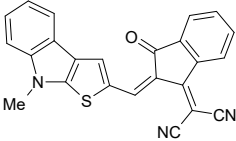


Figure 3. UV-vis absorption (left) and fluorescence (right) spectra of the TI-dyes in CHCl_3 solutions **2-4**.

Absorption maxima (λ_{\max}) of the studied compounds are successively red-shifted going from dye (**2**) to dye (**4**), reflecting the increase in ICT in the subsequent structures. Thus, the acceptor moiety of dye (**4**) causes the most significant bathochromic shift of the absorption band due to its strong electron-withdrawing nature. At the same time, an electron-deficient fragment of dye (**4**) has the more π -extended structure when compared with the structures of acceptor moieties in dyes (**2**) and (**3**). This fact also favors a more efficient intramolecular charge-transfer processes. The optical band gaps (E_g^{opt}) of dyes **2-4** have been calculated on the basis of the absorption-edge values (λ_{onset}); these compounds possess a narrow band gap of 2.03 eV, 1.91 eV and 1.69 eV, respectively. The data obtained are also presented in Table 1.

Table 1. Optical data for dyes **2-6**

Dye	λ_{\max} (nm)	λ_{onset} (nm)	λ_{em} (nm)	Stokes shift nm (cm^{-1})	E_g^{opt} (eV)*	ϵ ($\text{M}^{-1}\times\text{cm}^{-1}$)	
2	243,					20448, 9810,	 5 (MTI-DCV) ¹⁴
	288,	612	632	95 (2799)	2.03	6494, 37120	
	336, 537						
3	249,					31128,	 6 (MTI-DCI) ¹⁴
	294,	647	671	101 (2640)	1.91	10565, 8159,	
	349, 570					29100	
4	242,					27572,	
	321,	732	766	127 (2594)	1.69	28486,	
	369, 639					10409, 21835	
5	452				2.38	62000	
6	566				1.86	71000	

* $E_g^{\text{opt}} = 1240/\lambda_{\text{onset}}$

Thiophene is one of the most commonly used π -spacers for *push-pull* molecules which are among the most important building blocks for organic electronics materials, since its planar structure allows extended π -conjugation in a system. Our investigation has confirmed that incorporation of a thiophene moiety between electron-excessive and electron-deficient parts of a corresponding chromophore, e.g., compounds (**5**) and (**6**) (Table 1), results in significant changes in the dye's absorption spectrum, including red shifts of the major absorbance peaks, and absorption-edge values. These changes can be clearly seen if one compares the spectral data of two pairs of dyes, i.e., (**2**) and (**5**)¹⁴ and (**4**) and (**6**).¹⁴ It is important to notice that, in our case, the absorption intensity falls. At the same time, the influence of an alkyl substituent at the thieno[2,3-*b*]indole nitrogen atom cannot be excluded. In the case of compounds (**2**) and (**4**), the +I inductive effect of a 2-ethylhexyl chain enhances the basicity of the thieno[2,3-*b*]indole group to a greater extent than does a methyl group [compounds (**5**) and (**6**)].

The electrochemical behavior of all obtained compounds was estimated by cyclic voltammetry (CV) in the 1:1 mixture of dry MeCN and CH_2Cl_2 containing Et_4NClO_4 (0.23 g, 10^{-3} mol) as the supporting electrolyte. (The concentration of the compounds was fixed at 1×10^{-3} M to avoid aggregation.) A more detailed description of the CV experiment is presented in the Experimental Section. Some examples of the obtained cyclic voltammograms are displayed in Figure 4. Each CV curve shows two irreversible oxidation waves with oxidation-peak potentials (E_{ox}^1 , E_{ox}^2), the values of which depend on the nature of the electron-withdrawing

group. The values of oxidation potentials, as well as the values of the onset oxidation potentials ($E_{\text{ox onset}}$), are summarized in Table 2. The presence of the strong electron-accepting group in a dye molecule leads to the expected positive shift in the values of oxidation potentials. Therefore, the string of anodic peak potentials (E_{ox}^2) associated with formation of a radical cation, are as follows: 1.59 V (**2**), 1.62 V (**3**), 1.73 V (**4**).

HOMO and LUMO energy-level values, determined from experimental cyclic voltammetry, theoretical calculations, and band gap energy values found from UV-vis measurements, are summarized in Table 2.

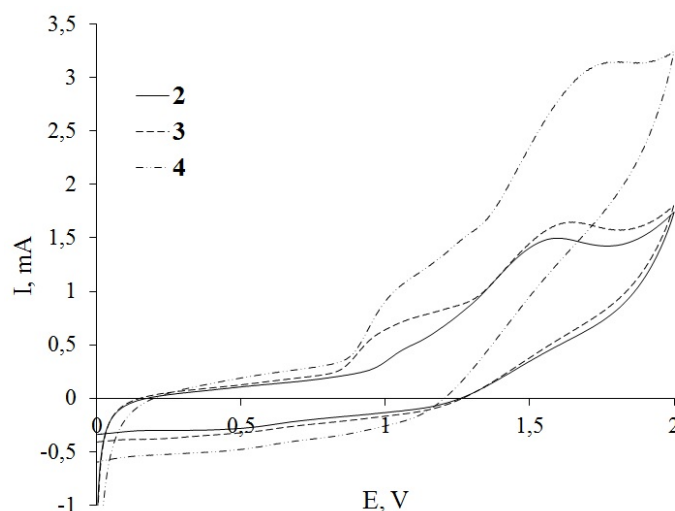


Figure 4. Comparison of CV curves of the dyes **2-4** ($\text{CH}_3\text{CN}/\text{CH}_2\text{Cl}_2$, Et_4NClO_4 , 10^{-3}M , 50 mV/s, 1st cycle).

The empirical HOMO and LUMO energy levels ($E_{\text{HOMO, cv}}$; $E_{\text{LUMO, cv}}$) of the dyes **2-4** were obtained using the equations¹⁵ presented in Supplementary Material Section.

It should be noted that the optical and electrical characteristics of compounds **2-4** are comparable with those of known organic dyes such as **NTU-2** dyes.¹² Dyes **2-4** possess sufficiently high molar-absorption coefficients in the visible light region (Table 1), which is one of the most important and necessary characteristics of the light-harvesting materials for solar-cell applications. In addition, their HOMO levels (Table 2) are lower than the value of the indium-tin oxide function (WF) (-4.7 eV),¹⁶ which is a conductive layer in HSC photoanodes. This makes the regeneration of oxidized dye molecules, after injection of excited electrons into an acceptor layer, possible. The latter process is energetically permitted for [6,6]-phenyl-C61-butyric acid methyl ester (PCBM-60), which is one of the most commonly used electron-acceptor materials for HSC, since LUMO energy levels of dyes **2-4** (Table 2) are higher than the LUMO level (-3.7 eV) of PCBM-60.¹⁷

Table 2. Electrochemical data of dyes **2-4**

Dye	E_{ox}^1 , V	E_{ox}^2 , (V)	$E_{\text{ox onset}}$ (V)	$E_{\text{HOMO, cv}}$ (eV)	$E_{\text{LUMO, cv}}$ (eV)	$E_{\text{HOMO, th}}$ (eV)	$E_{\text{LUMO, th}}$ (eV)	$E_{\text{gap, th}}$ (eV)	$E_{\text{g}}^{\text{opt}}$ (eV)
2	1.07	1.59	0.94	-5.33	-3.28	-5.65	-3.01	2.64	2.03
3	1.18	1.62	0.82	-5.21	-3.37	-5.36	-2.77	2.59	1.91
4	1.26	1.73	0.87	-5.26	-3.59	-5.55	-3.24	2.30	1.69

In order to obtain additional information on the electronic structure of compounds **2-4**, quantum chemical calculations of the energy and geometry of their frontier molecular orbitals have been performed using the

FireFly package.¹⁸ Geometries of all compounds have been fully optimized without symmetry constraints at the density-functional theory (DFT) (B3LYP)¹⁹⁻²² level with the Def2-TZVP basis set.²³ It becomes clear that electronic distribution of the HOMO of compounds **2-4** is delocalized over the entire molecule with the exception of a phenylene unit in compounds (**3**) and (**4**). The LUMO orbitals are delocalized substantially over the acceptor moieties and thiophene spacer of compounds, and partially over the thiophene unit of a thieno[2,3-*b*]indole moiety (Figures 5-7).

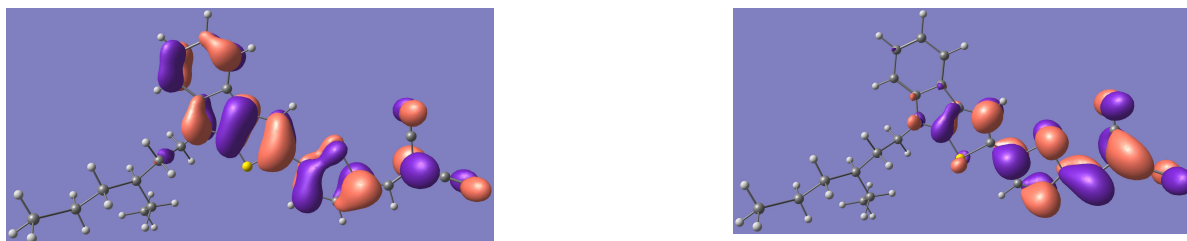


Figure 5. Calculated HOMO and LUMO electron density of dye (**2**).



Figure 6. Calculated HOMO and LUMO electron density of dye (**3**).



Figure 7. Calculated HOMO and LUMO electron density of dye (**4**).

The calculated energies of HOMO and LUMO ($E_{\text{HOMO, th}}$; $E_{\text{LUMO, th}}$) listed in Table 2 are rather close to the values obtained through the cyclic-voltammetry measurements. The calculated HOMO levels were 0.15-0.32 eV lower than the experimentally obtained levels, whereas the calculated LUMO levels were 0.27-0.4 eV higher. Compound (**4**) shows the smallest energy gap (2.3 eV) while compound (**2**) shows the largest (2.64 eV) energy gap. The calculated values of energy gaps ($E_{\text{gap, th}}$) are also in agreement with the $E_{\text{g}}^{\text{opt}}$ values obtained from the UV-Vis data.

Conclusions

In summary, we have synthesized and characterized three new push-pull organic dyes bearing the thieno[2,3-*b*]indole electron-excessive system and three different electron-withdrawing fragments. The main spectral and

electrochemical characteristics of these compounds have been elucidated, and these data have been used to estimate their HOMO / LUMO energy levels and energy-band gaps. It has been found that the dyes possess narrow band gaps of 2.03 eV, 1.91 eV and 1.69 eV, respectively, and an effective absorption in the visible spectral region. The absorption maxima of their UV-spectra are located in the range of 440-740 nm. Therefore, the obtained push-pull chromophores can be considered promising light-harvesting materials for planar as well as bulk heterojunction solar cells. Further studies are in progress.

Experimental Section

General. ^1H and ^{13}C NMR spectra were recorded on a Bruker Avance III HD 400 (400 MHz) spectrometer in CDCl_3 with hexamethyldisiloxane (0.055 ppm) as an internal standard. Elemental analysis was carried out using a CHNS-932 LECO Corp analyzer. IR spectra were recorded on a Spectrum Two FTIR spectrometer (Perkin Elmer) for chloroform solutions of the samples. Reaction course and purity of both starting and resulting compounds were monitored by thin-layer chromatography on Sorbfil plates. The mixtures were separated and target products purified using column chromatography on silica gel (Lancaster, Silica Gel 60, 0.060–0.2 mm). Mass spectra of the starting compounds were recorded on an Agilent Technologies 6890N/5975B instrument (ionization electron energy 70 eV). UV-Vis absorption spectra were recorded for chloroform solutions of compounds in 10 mm cuvettes using a Shimadzu UV-2600 spectrophotometer. Fluorescence spectra were recorded using a Shimadzu RF-5301 PC spectrofluorophotometer (excitation wavelength 220 nm, cuvette dimensions 10×10 mm, solvent - dried CHCl_3). Electrochemical measurements were carried out on a potentiostat/galvanostat (ZRA Interface 1000) using a three-electrode cell with carbon-pyroceramic working electrode, a Pt wire counter electrode, and a Ag/Ag^+ reference electrode in a 0.1 M solution of Et_4NClO_4 in acetonitrile-dichloromethane mixture (1:1, v/v). Potential scan rate was 50 mV/s.

Quantum chemical calculations of molecular orbital energies using B3LYP/6-31G(d) were performed using the Firefly software on a PGU Tesla supercomputer.

2-(3-Oxo-2,3-dihydroindene-1-ylidene)malononitrile was synthesized according to the synthetic procedure described in [11].

{[(8-(2-Ethylhexyl)-8H-thieno[2,3-b]indol-2-yl)]thiophen-2-ylmethylidene}propanedinitrile (2). The mixture of aldehyde (**1**) (198 mg, 0.5 mmol), $\text{CH}_2(\text{CN})_2$ (66 mg, 1 mmol) and pyrrolidine (0.02 ml) was heated under reflux in AcOH (5 ml) for 4 h, then cooled and diluted with MeOH (10 ml). The resulting solid was filtered off, washed with MeOH and dried, affording the dye (**2**) as a black powder. Yield: 156 mg (70%), mp 104–106 °C. IR, cm^{-1} : 2222 ($\text{C}\equiv\text{N}$) (CHCl_3). ^1H NMR (CDCl_3 , 400 MHz) δ : 0.82 (3H, t, $^3J_{\text{HH}}$ 8 Hz), 0.89 (3H, t, $^3J_{\text{HH}}$ 7.5 Hz) 1.34 (8H, m), 2.08 (1H, m), 4.04 (2H, d, $^3J_{\text{HH}}$ 7.5 Hz), 7.16 (1H, d, $^3J_{\text{HH}}$ 4.2 Hz), 7.19 (1H, t, $^3J_{\text{HH}}$ 8.0 Hz), 7.27 (1H, d, $^3J_{\text{HH}}$ 8.3 Hz), 7.31 (1H, t, $^3J_{\text{HH}}$ 8.0 Hz), 7.50 (1H, d, $^3J_{\text{HH}}$ 4.2 Hz), 7.74 (1H, s), 7.76 (1H, d, $^3J_{\text{HH}}$ 7.8 Hz). ^{13}C NMR (CDCl_3 , 400 MHz,) δ = 10.6, 13.9, 22.6, 24.2, 28.7, 31.9, 39.1, 50.7, 74.1, 109.7, 113.8, 114.7, 119.2, 122.4, 123.2, 125.9, 129.8, 130.8, 131.8, 140.4, 141.0, 142.7, 146.3, 147.0, 149.5, 152.0. Anal. calcd. for $\text{C}_{26}\text{H}_{25}\text{N}_3\text{S}_2$ (443.63): C, 70.39; H, 5.68; N, 9.47; S, 14.46. Found: C, 70.32; H, 5.65; N, 9.53; S, 14.41 %.

2-({5-[8-(2-Ethylhexyl)-8H-thieno[2,3-b]indol-2-yl]thiophen-2-yl}methylidene)-2,3-dihydro-1H-indene-1,3-dione (3). 1,3-Indanedione (40 mg, 0.30 mmol,) and aldehyde (**1**) (90 mg, 0.25 mmol) were dissolved in *n*-butanol (3ml). After 3 h of reflux, the reaction mixture was cooled down to room temperature. The crude product was filtered off and purified by column chromatography (silica gel, eluent – mixture $\text{CH}_2\text{Cl}_2/\text{Hex}$, 1:1) to get the desired compound (**3**) as a purple solid, yield 90 mg (68%). M.p. 115–117 °C. IR, cm^{-1} : 1716 ($\text{C}=\text{O}$)

(CHCl₃). ¹H NMR (CDCl₃, 400 MHz) δ: 0.80 (3H, t, ³J_{HH} 7.3 Hz), 0.92 (3H, t, ³J_{HH} 7.6 Hz), 1.27 (8H, m), 2.11 (1H, m), 4.05 (2H, d, ³J_{HH} 7.5 Hz), 7.18 (1H, t, ³J_{HH} 8.0 Hz), 7.26 (1H, d, ³J_{HH} 8.4 Hz), 7.31 (1H, t, ³J_{HH} 8.1 Hz), 7.38 (1H, d, ³J_{HH} 8.3 Hz), 7.69-7.72 (2H, m), 7.77 (1H, d, ³J_{HH} 7.6 Hz), 7.80 (1H, s), 7.83 (1H, d, ³J_{HH} 4.1 Hz), 7.73 (s, 1H), 7.91 (2H, m). ¹³C NMR (CDCl₃, 400 MHz) δ = 10.6, 13.9, 22.6, 24.2, 28.6, 31.8, 39.1, 50.7, 119.7, 116.7, 119.9, 120.2, 121.9, 122.5, 122.7, 125.1, 127.2, 128.8, 132.6, 134.5, 134.7, 135.3, 136.1, 137.8, 140.5, 141.9, 142.6, 144.0, 151.4, 154.6, 158.8, 188.5, 192.5. Anal. calcd. for C₃₂H₂₉NO₂S₂ (523.71): C, 73.39; H, 5.58; N, 2.67; S, 12.25. Found: C, 73.36; H, 5.53; N, 2.71; S, 12.15 %.

2-[2-({5-[8-(2-Ethylhexyl)-8H-thieno[2,3-b]indol-2-yl]thiophen-2-yl}methylenidene)-3-oxo-2,3-dihydro-1H-inden-1-ylidene]propanedinitrile (4). 3-(Dicyanomethylene)indan-1-one (30 mg, 0.18 mmol) was added to a solution of aldehyde (**1**) (100 mg, 0.25 mmol) in ethanol (6 ml) at 60 °C. The reaction mixture was then stirred for 5 min, cooled down to room temperature, concentrated *in vacuo* and purified by chromatography on silica gel (eluent: CH₂Cl₂/Hex, 1:1) to get the desired compound as a dark blue solid, yield 80 mg (56 %). M.p. 194-196 °C. IR, cm⁻¹: 2220 (C≡N), 1690 (C=O) (CHCl₃). ¹H NMR (CDCl₃, 400 MHz)ppm: 0.86 (3H, t, ³J_{HH} 8), 0.91 (3H, t, ³J_{HH} 7.6), 1.36 (8H, m), 2.11 (1H, m), 4.04 (2H, d, ³J_{HH} 7.5 Hz), 7.20 (1H, t, ³J_{HH} 8.4 Hz), 7.26 (1H, d, ³J_{HH} 4.2 Hz), 7.32 (1H, t, ³J_{HH} 8.0 Hz), 7.38 (1H, d, ³J_{HH} 8.8 Hz), 7.68 (2H, t, ³J_{HH} 9.6 Hz), 7.73 (1H, d, ³J_{HH} 4.4 Hz), 7.84 (2H, d, ³J_{HH} 8.0 Hz), 7.88 (1H, s), 8.63 (2H, d, ³J_{HH} 8.0 Hz), 8.78 (1H, s). ¹³C NMR (CDCl₃, 400 MHz) δ = 10.5, 14.0, 22.9, 24.2, 29.3, 31.8, 38.9, 50.6, 76.4, 112.1, 113.7, 116.3, 120.0, 122.1, 123.4, 124.2, 125.5, 125.9, 128.0, 128.7, 130.8, 132.2, 134.1, 134.7, 135.6, 140.4, 143.7, 146.8, 149.5, 153.8, 156.8, 158.7, 159.7, 167.6, 190.9. Anal. calcd. for C₃₅H₂₉N₃OS₂ (571.75): C, 73.52; H, 5.11; N, 7.35; S, 11.22. Found: C, 73.49; H, 5.07; N, 7.27; S, 11.16 %.

Acknowledgements

This research study was financially supported by the Russian Science Foundation (Project No. 16-13-10435).

References

- Wetzel, C.; Mishra, A.; Mena-Osteritz, E.; Walzer, K.; Pfeiffer, M.; Bäuerle, P. *J. Mater. Chem. C* **2016**, *4*, 3, <https://doi.org/10.1039/C5TC03539B>
- Wang, K.; Azouz, M.; Babics, M.; Cruciani, F.; Marszalek, T.; Saleem, Q.; Pisula, W.; Beaujuge, P. M. *Chem Mater* **2016**, *28*, 5415. <https://doi.org/10.1021/acs.chemmater.6b01763>
- Cho, I.; Jeon, N. J.; Kwon, O. K.; Kim, D. W.; Jung, E. H.; Noh, J. H.; Seo, J.; Seok, I. S.; Park, S. Y. *Chem. Sci* **2017**, *8*, 734. <https://doi.org/10.1039/C6SC02832B>
- Irgashev, R. A.; Karmatsky, A. A.; Rusinov, G. L.; Charushin, V. N. *Org. Lett* **2016**, *18*, 804. <https://doi.org/10.1021/acs.orglett.6b00081>
- Zhao, B.; Yan, C.; Wang, Z.; Huang, H.; Hu, Y.; Cheng, P.; Yi, M.; Huang, C.; Zhan, X.; Huang, W. *J. Mater. Chem. C* **2017**, *5*, 8988. <https://doi.org/10.1039/C7TC02912H>
- Wang, Z.-S.; Koumura, N.; Cui, Y.; Takahashi, M.; Sekiguchi, H.; Mori, A.; Kubo, T.; Furube, A.; Hara, K. *Chem. Mater* **2008**, *20*, 3993.

- <https://doi.org/10.1021/cm8003276>
7. Koumura, N.; Wang, Z.-S.; Miyashita, M.; Uemura, Y.; Sekiguchi, H.; Cui, Y.; Mori, A.; Mori, S.; Hara, K. *J. Mater. Chem.* **2009**, *19*, 4829.
<https://doi.org/10.1039/b905831a>
 8. Zhang, X.-H.; Cui, Y.; Katoh, R.; Koumura, N.; Hara, K. *J. Phys. Chem. C* **2010**, *114*, 18283.
<https://doi.org/10.1021/jp105548u>
 9. Irgashev, R. A.; Karmatsky, A. A.; Rusinov, G. L.; Charushin, V. N. *Beilstein J. Org. Chem.* **2015**, *11*, 1000.
<https://doi.org/10.3762/bjoc.11.112>
 10. Irgashev, R. A.; Karmatsky, A. A.; Kozyukhin, S. A.; Ivanov, V. K.; Sadovnikov, A.; Kozik, V. V.; Grinberg, V. A.; Emets, V. V.; Rusinov, G. L.; Charushin, V. N. *Synth. Met.* **2015**, *199*, 152.
<https://doi.org/10.1016/j.synthmet.2014.11.024>
 11. Irgashev, R. A.; Karmatsky, A. A.; Kim, G. A.; Sadovnikov, A. A.; Emets, V. V.; Grinberg, V. A.; Ivanov, V. K.; Kozyukhin, S. A.; Rusinov, G. L.; Charushin, V. N. *Arkivoc.* **2017**, *iv*, 34.
<http://dx.doi.org/10.3998/ark.5550190.p009.887>
 12. Zhang, T.; Han, H.; Zou, Y.; Lee, Y.-C.; Oshima, H.; Wong, K.-T.; Holmes, R. *J. ACS. Appl. Mater. Interfaces.* **2017**, *9*, 25418.
<https://doi.org/10.1021/acsami.7b05304>
 13. Kim, B.-S.; Yu, H.; Son, Y.-A. *Mol. Cryst. Liq. Cryst.* **2012**, *563*, 257.
<https://doi.org/10.1080/15421406.2012.689733>
 14. Baert, F.; Cabanetos, C.; Allain, M.; Silvestre, V.; Leriche, P.; Blanchard, P. *Org. Lett.* **2016**, *18*, 1582.
<https://doi.org/10.1021/acs.orglett.6b00438>
 15. Shiao, S.-Y.; Chang, C.-H.; Chen, W.-Y.; Wang, H.-J.; Jeng, R.-J.; Lee, R.-H. *Dyes Pigm.* **2015**, *115*, 35.
<https://doi.org/10.1016/j.dyepig.2014.12.007>
 16. Park, Y.; Choong, V.; Gao, Y.; Hsieh, B. R.; Tang, C. W. *Appl. Phys. Lett.* **1996**, *68*, 2699.
<https://doi.org/10.1063/1.116313>
 17. Kinoshita, Y.; Takenaka, R.; Murata, H. *Appl. Phys. Lett.* **2008**, *92*, 243309.
<https://doi.org/10.1063/1.2949321>
 18. Granovsky, A. A. Firefly, version 8
<http://classic.chem.msu.su/gran/firefly/index.html>
 19. Parr, R. G.; Yang, W. *Density-functional theory of atoms and molecules*, Oxford: University Press, 1989; p 333
 20. Becke, A. D. *J. Chem. Phys.*, **1993**, *98*, 5648.
<https://doi.org/10.1063/1.464913>
 21. Lee, C.; Yang, W.; Parr, R. G. *Phys. Rev. B* **1988**, *37*, 785.
<https://doi.org/10.1103/PhysRevB.37.785>
 22. Hehre, W. J.; Radom, L.; Schleyer, P. R.; Pople, J. A. *AB INITIO Molecular Orbital Theory*, Wiley: New York; 1986, p 576
 23. Weigend, F.; Ahlrichs, R. *Phys. Chem. Chem. Phys.* **2005**, *7*, 3297.
<https://doi.org/10.1039/b508541a>
 24. Bello, K. A.; Cheng, L.; Griffiths, J., *J. Chem. Soc. Perkin. Trans. II* **1987**, 815.
<https://doi.org/10.1039/p29870000815>
 25. Irick, G., *J. J. Chem. Eng. Data*, **1971**, *16*, 118.
<http://dx.doi.org/10.1021/jc60048a040>